Infrared emission spectra of BeH and BeD

A. Shayesteh, K. Tereszchuk, and P. F. Bernath[a)]
Department of Chemistry, University of Waterloo, Waterloo, Ontario N2L 3G1, Canada

R. Colin
Laboratoire de Chimie Physique Moléculaire, Université Libre de Bruxelles, C.P. 160/09, 50 av. F.D. Roosevelt, 1050 Brussels, Belgium

(Received 8 August 2002; accepted 22 October 2002)

High resolution infrared emission spectra of beryllium monohydride and monodeuteride have been recorded. The molecules were generated in a furnace-discharge source, at 1500 °C and 333 mA discharge current, with beryllium metal and a mixture of helium and hydrogen or deuterium gases. Approximately 160 BeH lines and 167 BeD lines for the vibrational bands $v=1\rightarrow0$ to $v=4\rightarrow3$ were observed in the spectra and spectroscopic constants were determined. The Dunham constants ($Y_{l,m}$) and Born–Oppenheimer breakdown constants were obtained in a combined fit of the BeH and BeD data. The equilibrium rotational constants (B_e) for BeH and BeD were found to be 10.319 59(3) cm^{-1} and 5.688 29(2) cm^{-1}, respectively, while the equilibrium vibrational constants (ω_e) are 2061.416(3) and 1529.956(3) cm^{-1}. The equilibrium distance (R_e) was determined to be 1.342 436(2) Å for BeH. [DOI: 10.1063/1.1528606]

INTRODUCTION

The BeH molecule is one of the lightest diatomics with only five electrons. BeH is, therefore, a popular target for *ab initio* calculations and is often used to test new methods for open-shell systems.[1,2] Because beryllium-containing compounds are highly toxic,[3] BeH has been less studied experimentally. The previous work on BeH and BeD was recently reviewed by Focsa *et al.*,[4,5] who measured new high resolution emission spectra of the $A\,^2\Pi-X\,^2\Sigma^+$ transitions of BeH and BeD with a Fourier transform spectrometer. Since this work was published in 1998, no new experimental results have been reported, but a number of theoretical papers have been published. For example, a new ground state potential energy curve of BeH was calculated by Martin[6,7] using high level *ab initio* methods. Machado *et al.*[8] have calculated transition dipole moment functions and radiative transition probabilities for $A\,^2\Pi-X\,^2\Sigma^+$ and $C\,^2\Sigma^+-X\,^2\Sigma^+$ systems of BeH, and some calculations on the nature of the Rydberg states have been carried out.[9,10] In spite of this considerable interest in BeH, no vibration–rotation or pure rotation spectrum has been recorded. The existing infrared spectrum is based on BeH trapped in an argon matrix.[11] We have now recorded the first vibration–rotation spectrum of gaseous BeH and BeD. The spectra were recorded in emission using a new molecular source that combines a high temperature furnace with an electrical discharge.

EXPERIMENTAL DETAILS

The high resolution infrared emission spectra of BeH and BeD were recorded with a Bruker IFS 120 HR Fourier transform spectrometer. A new emission source with an electrical discharge inside a high temperature furnace was used to make the molecules. Powdered beryllium metal (about 5 g) was placed inside a zirconia boat in the center of an alumina tube (5 cm×120 cm). The central part of the tube was heated to 1500 °C by a CM Rapid Temp furnace, and the end parts were cooled by water and sealed with CaF_2 windows. A slow flow of helium (about 20 Torr) and hydrogen or deuterium (a few Torr) was passed through the cell. Two stainless steel tube electrodes were placed inside the cool ends of the tube, and a dc discharge (2.5 kV, 333 mA) was struck between them. A CaF_2 lens was used to focus the emitted light from the source into the entrance aperture of the spectrometer.

Two spectra for BeH and BeD were recorded in the 16 000–32 000 cm^{-1} (visible) region using a visible quartz beamsplitter and a photomultiplier tube detector. In these spectra we observed the $A\,^2\Pi-X\,^2\Sigma^+$ transitions, and we optimized the experimental conditions to obtain the best signal. We then switched to a CaF_2 beamsplitter, evacuated the spectrometer and changed the detector to either InSb or HgCdTe.

A BeD spectrum was recorded in the spectral region of 1200–2200 cm^{-1} at an instrumental resolution of 0.03 cm^{-1} using a liquid nitrogen-cooled HgCdTe (MCT) detector, and 200 scans were added. The spectral bandpass was set by the CaF_2 beamsplitter and a 2200 cm^{-1} longwave pass filter.

Two BeH spectra were recorded (200 scans each): the first one with the same conditions as for BeD, but for the second one we used a liquid nitrogen-cooled InSb detector in the spectral region of 1800–2900 cm^{-1}. In this case the bandpass was set by the detector and a 2900 cm^{-1} longwave pass filter. Atomic and molecular emission lines were present in the spectra, as well as absorption lines from atmospheric CO_2 and H_2O. The signal-to-noise ratio for the strongest BeH lines was about 350.

a)Author to whom all correspondence should be addressed; electronic mail: bernath@uwaterloo.ca

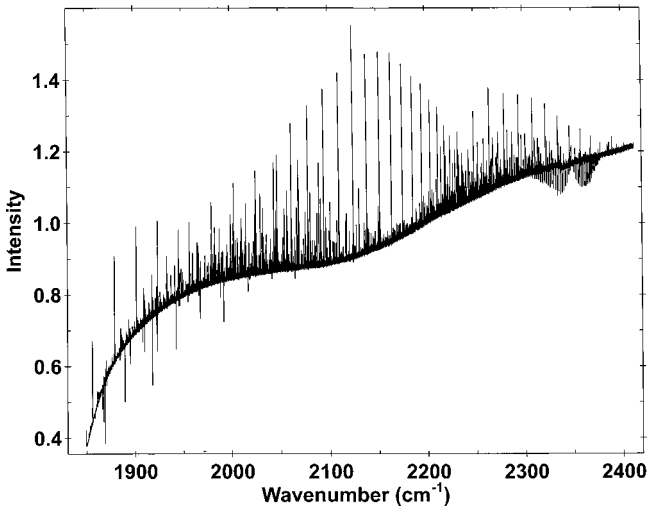

FIG. 1. An overview of the infrared emission spectrum of BeH recorded with the InSb detector. Nearly all emission lines above 2240 cm^{-1} are from BeH_2. The absorption of atmospheric CO_2 can be seen near 2350 cm^{-1}.

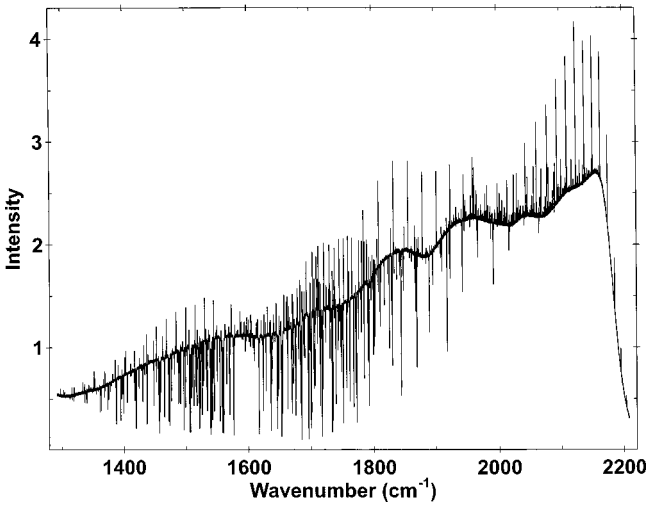

FIG. 3. An overview of the infrared emission spectrum of BeH recorded with the HgCdTe detector. The absorption lines are from atmospheric H_2O.

RESULTS AND DISCUSSION

The strongest emission lines in the overview spectrum recorded with the InSb detector (Fig. 1) are the *R* branch lines of the BeH $v=1\rightarrow0$ band. Nearly all of the emission lines above 2240 cm^{-1}, and many lines in the 1900–2200 cm^{-1} region are from the antisymmetric stretching mode ν_3 (and several hot bands) of BeH_2.[12] Atmospheric CO_2 absorption lines can be seen near 2350 cm^{-1}. An expanded portion of the *R* branch of the fundamental band of BeH is shown in Fig. 2. This spectrum had channeling in the baseline that we could not eliminate in spite of our efforts. Most of *P* branch lines fell below the 1800 cm^{-1} cutoff of InSb detector and had to be recorded with the MCT detector. The overview spectrum in the MCT region (Fig. 3) contained many *P* branch lines, as well as strong atmospheric H_2O absorption. All of the BeD lines fell in the MCT region. The strongest emission lines in the BeD spectrum (Fig. 4) are from BeD $v=1\rightarrow0$ band, and nearly all the emission lines above 1680 cm^{-1} are from the antisymmetric stretching mode ν_3 (and a few hot bands) of BeD_2.[12]

Line positions in the spectra were determined using the WSPECTRA program from Carleer (Université Libre de Bruxelles). The BeH spectra were calibrated using impurity CO emission lines, and the BeH lines (EPAPS[13]) have an absolute accuracy of better than 0.001 cm^{-1}. The calibration of BeD spectrum was based on five common lines in the BeH and BeD spectra in the 1200–2200 cm^{-1} region. The spectra of both BeH and BeD contained the fundamental $v=1\rightarrow0$ band, as well as three hot bands: 2–1, 3–2, and 4–3. Assignment of the bands was carried out using a color Loomis–Wood program.

The ground state of beryllium monohydride is $X\,^2\Sigma^+$ state, but no spin-splitting was observed in the spectra, and the lines were fitted using a $^1\Sigma^+$ state energy level expression using Le Roy's DSPARFIT program.[14] The spectroscopic

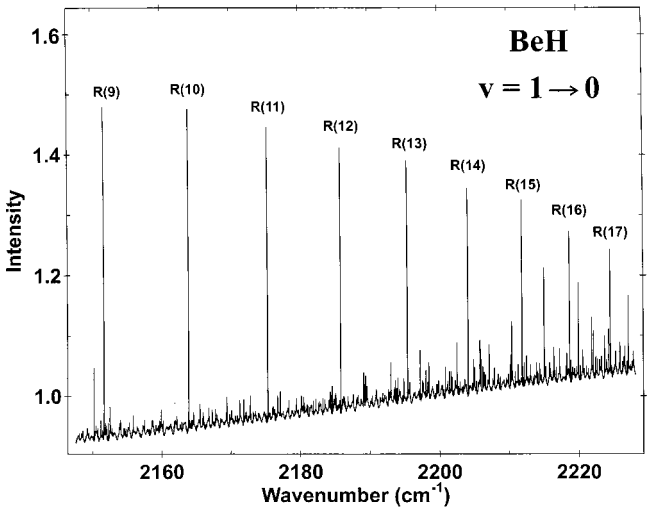

FIG. 2. An expanded view of the *R* branch of BeH $v=1\rightarrow0$ band. The weak lines are from BeH_2.

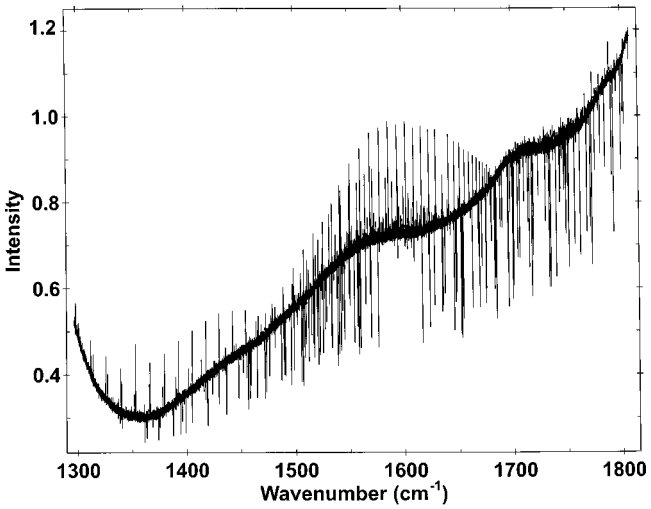

FIG. 4. An overview of the infrared emission spectrum of BeD recorded with the HgCdTe detector. Nearly all emission lines above 1680 cm^{-1} are from BeD_2.

TABLE I. Spectroscopic constants (in cm^{-1}) for the $X\,^2\Sigma^+$ ground state of BeH (all uncertainties are 2σ).

Parameter	$v=0$	$v=1$	$v=2$	$v=3$	$v=4$
T_v	0.0	1986.4158(4)	3896.8702(5)	5729.2615(6)	7480.3404(16)
B_v	10.165 613(23)	9.855 737(21)	9.541 635(21)	9.220 120(21)	8.886 589(46)
$D_v\times10^3$	1.026 41(16)	1.016 24(14)	1.009 82(13)	1.008 85(13)	1.016 05(34)
$H_v\times10^8$	10.081(39)	9.756(35)	9.327(31)	8.756(30)	7.921(67)
$L_v\times10^{11}$	−1.197(32)	−1.258(28)	−1.368(24)	−1.605(21)	−2.0[a]

[a]Fixed value. This value was determined by extrapolation of L_v, $v=0-3$.

constants in Tables I and II for both molecules were determined by fitting the lines to the customary expression for rotational energy levels:

$$E_{vN}=T_v+B_vN(N+1)-D_v[N(N+1)]^2+H_v[N(N+1)]^3+L_v[N(N+1)]^4. \quad (1)$$

BeH lines were also fitted using the Dunham energy expression,

$$E_{vN}^{\mathrm{BeH}}=\sum_{l,m} Y_{l,m}^{\mathrm{BeH}}\left(v+\frac{1}{2}\right)^l[N(N+1)]^m, \quad (2)$$

to yield the constants given in Table III. In this fit both isotopomers were included, and Born–Oppenheimer breakdown constants were derived. The Dunham constants of two isotopomers of the $A-B$ molecule are related via[14]

$$Y_{l,m}^{\alpha}=\left\{Y_{l,m}^{1}+\frac{\Delta M_A^{\alpha}}{M_A^{\alpha}}\delta_{l,m}^{A}+\frac{\Delta M_B^{\alpha}}{M_B^{\alpha}}\delta_{l,m}^{B}\right\}\left(\frac{\mu_1}{\mu_{\alpha}}\right)^{m+l/2}. \quad (3)$$

The δ's are the Born–Oppenheimer breakdown parameters for the atoms A and B with masses M_A and M_B, and μ's are reduced masses. The index 1 is for the main (reference) isotopomer and α is the index for the other isotopomer(s).

In the BeH/D case, Eq. (3) is simpler because beryllium has only one naturally occurring isotope $^9_4$Be:

$$Y_{l,m}^{\mathrm{BeD}}=\left\{Y_{l,m}^{\mathrm{BeH}}+\frac{M_{\mathrm{D}}-M_{\mathrm{H}}}{M_{\mathrm{D}}}\delta_{l,m}^{\mathrm{H}}\right\}\left(\frac{\mu_{\mathrm{BeH}}}{\mu_{\mathrm{BeD}}}\right)^{m+l/2}. \quad (4)$$

The Dunham constants for BeD in Table III are derived by calculation from the BeH constants and the Born–Oppenheimer breakdown constants ($\delta_{l,m}^{\mathrm{H}}$). The technique of sequential rounding and refitting[15] has been applied to the constants of Table III to minimize the number of digits. Of course, the derived Dunham constants for BeD (Table III) will require more digits as determined by the parameter sensitivities.[15]

The new BeH constants are in good agreement with the *ab initio* calculations by Martin.[7] In those calculations, he included the adiabatic correction (diagonal correction to the Born–Oppenheimer approximation) to the energy and obtained equilibrium constants close to the experimental ones. The nonadiabatic correction, which is of equal significance, was not included in his calculations. Our constants for BeH differ substantially from the previous experimental constants of Focsa *et al.*[4] (See Table IV). There are three reasons for such differences.

(1) The precision of our infrared data is better than 0.001 cm^{-1}, compared to 0.01 cm^{-1} in the previous FTS spectrum of the $A\,^2\Pi-X\,^2\Sigma^+$ transition.

(2) The vibrational intervals were determined by the $\Delta v=-1$ bands of the $A\,^2\Pi-X\,^2\Sigma^+$ transition in an old spectrum recorded with a small classical spectrograph with only moderate resolution. The uncertainty in the relative line positions was 0.1 cm^{-1}, and the absolute uncertainty was estimated to be 0.2 cm^{-1}.

(3) In the previous Dunham fit, all data for $v=0$ to $v=10$ of the ground state were fitted with an eighth-order polynomial for $Y_{l,0}$ constants and seventh order for $Y_{l,1}$. Presumably because of the presence of high-order terms in the Dunham fit, the lower-order terms lost their physical significance.

In the BeD case, the agreement between the new constants and previous experimental constants[5] is more reasonable. However, the Dunham constants determined in the present work represent only the lower half of the potential well. In future work, we will include the previous $A\,^2\Pi-X\,^2\Sigma^{+}$[4,5] and $C\,^2\Sigma^+-X\,^2\Sigma^{+}$[16] data for both BeH and BeD in a direct potential fit for the ground state. In this work we will make a grand fit of all available data, discuss the Born–Oppenheimer breakdown constants, and provide con-

TABLE II. Spectroscopic constants (in cm^{-1}) for the $X\,^2\Sigma^+$ ground state of BeD (all uncertainties are 2σ).

Parameter	$v=0$	$v=1$	$v=2$	$v=3$	$v=4$
T_v	0.0	1488.8426(5)	2936.1897(7)	4341.3758(9)	5703.4618(25)
B_v	5.625 285(31)	5.498 876(31)	5.371 486(32)	5.242 539(33)	5.111 211(59)
$D_v\times10^4$	3.1290(21)	3.1041(23)	3.0845(24)	3.0729(24)	3.0688(36)
$H_v\times10^8$	1.755(72)	1.716(74)	1.663(72)	1.617(66)	1.516(81)
$L_v\times10^{12}$	−2.06(98)	−1.95(86)	−1.85(74)	−1.90(62)	−1.77(61)

TABLE III. Dunham and Born–Oppenheimer breakdown constants (in cm^{-1}) for the $X\,^2\Sigma^+$ ground state of BeH and BeD (all uncertainties are 2σ).

	BeH	BeD
$Y_{1,0}$	2061.416 26(260)	1529.955 626
$Y_{2,0}$	−37.433 4(22)	−20.497 223 2
$Y_{3,0}$	0.032 5(7)	−0.018 668 8
$Y_{4,0}$	−0.047 84(8)	−0.011 505 73
$Y_{0,1}$	10.319 59(3)	5.688 286 3
$10^3\,Y_{1,1}$	−307.474 4(330)	−125.901 363
$10^3\,Y_{2,1}$	−0.942 8(260)	−0.163 156
$10^3\,Y_{3,1}$	−0.071 7(84)	−0.049 292 2
$10^3\,Y_{4,1}$	−0.057 9(9)	−0.006 663 7
$10^6\,Y_{0,2}$	−1032.84(20)	−314.292 09
$10^6\,Y_{1,2}$	13.953(150)	3.175 25
$10^6\,Y_{2,2}$	−2.022(90)	−0.337 579 3
$10^6\,Y_{3,2}$	0.188(26)	0.023 290 8
$10^6\,Y_{4,2}$	−0.054(3)	−0.004 964 25
$10^9\,Y_{0,3}$	102.64(51)	17.136 07
$10^9\,Y_{1,3}$	−4.23(34)	−0.524 044
$10^9\,Y_{2,3}$	0.678(86)	0.062 328 9
$10^9\,Y_{3,3}$	−0.202(12)	−0.013 779 8
$10^{12}\,Y_{0,4}$	−12.1(4)	−1.112 36
$10^{12}\,Y_{1,4}$	0.71(30)	0.048 434
$10^{12}\,Y_{2,4}$	−0.52(6)	−0.026 322 5
$\delta^{\mathrm{H}}_{1,0}$	0.766 8(79)	
$\delta^{\mathrm{H}}_{2,0}$	0.417 9(83)	
$\delta^{\mathrm{H}}_{3,0}$	−0.156 5(34)	
$\delta^{\mathrm{H}}_{4,0}$	0.019 8(5)	
$\delta^{\mathrm{H}}_{0,1}$	0.021 61(7)	
$10^3\,\delta^{\mathrm{H}}_{1,1}$	−1.311(42)	
$10^3\,\delta^{\mathrm{H}}_{2,1}$	0.81(4)	
$10^3\,\delta^{\mathrm{H}}_{3,1}$	−0.295(18)	
$10^3\,\delta^{\mathrm{H}}_{4,1}$	0.036(3)	
$10^6\,\delta^{\mathrm{H}}_{0,2}$	−7.49(25)	
$10^6\,\delta^{\mathrm{H}}_{1,2}$	0.32(4)	

stants suitable for the whole range of the potential well.

Most of the lines in our infrared spectra turned out to be due to BeH_2 or BeD_2. We have recently published a note on the detection of the ν_3 band of BeH_2.[17] The analysis of BeD_2 and BeH_2 hot bands has just been completed, and will be published separately.

TABLE IV. A comparison of equilibrium constants of BeH.

Constant	Martin[a]	Focsa *et al.*[b]	This work
ω_e (cm^{-1})	2062.119	2068.8634(5174)	2061.416 26(260)
$\omega_e x_e$ (cm^{-1})	36.938	46.145 5(6352)	37.433 4(22)
R_e (Å)	1.341 04	1.341 68(3)	1.3424 36(2)

[a]Reference 7.
[b]Reference 4.

ACKNOWLEDGMENTS

This work was supported by the Natural Sciences and Engineering Research Council (NSERC) of Canada and by the Fonds National de la Recherche Scientifique (FNRS) of Belgium. We thank R. J. Le Roy for help with DSPARFIT program.

[1] H. Meissner and J. Paldus, J. Chem. Phys. **113**, 2622 (2000).
[2] M. P. Fülscher and L. Serrano-Andrés, Mol. Phys. **100**, 903 (2002).
[3] S. Budavari, M. J. O'Neil, A. Smith, and P. E. Heckelman, *The Merck Index*, 11th ed. (Merck, New Jersey, 1989), pp. 181–183.
[4] C. Fosca, S. Firth, P. F. Bernath, and R. Colin, J. Chem. Phys. **109**, 5795 (1998).
[5] C. Fosca, P. F. Bernath, R. Mitzner, and R. Colin, J. Mol. Spectrosc. **192**, 348 (1998).
[6] J. M. L. Martin, Chem. Phys. Lett. **273**, 98 (1997).
[7] J. M. L. Martin, Chem. Phys. Lett. **283**, 283 (1998).
[8] F. B. C. Machado, O. Roberto-Neto, and F. R. Ornellas, Chem. Phys. Lett. **305**, 156 (1999).
[9] F. B. C. Machado, O. Roberto-Neto, and F. R. Ornellas, Chem. Phys. Lett. **284**, 293 (1998).
[10] I. D. Petsalakis, D. Papadopoulos, G. Theodorakopoulos, and R. J. Buenker, J. Phys. B **32**, 3225 (1999).
[11] T. J. Tague and L. Andrews, J. Am. Chem. Soc. **115**, 12111 (1993).
[12] A. Shayesteh, K. Tereszchuk, P. F. Bernath, and R. Colin, J. Chem. Phys. (submitted).
[13] See EPAPS Document No. E-JCPSA6-117-011303 for the observed line positions of the $v=1\rightarrow0$ to $v=4\rightarrow3$ bands of BeH and BeD. A direct link to this document may be found in the online article's HTML reference section. The document may also be reached via the EPAPS homepage (http://www.aip.org/pubservs/epaps.html) or from ftp.aip.org in the directory/epaps. See the EPAPS homepage for more information.
[14] R. J. Le Roy, J. Mol. Spectrosc. **194**, 189 (1999), http://leroy.uwaterloo.ca/.
[15] R. J. Le Roy, J. Mol. Spectrosc. **191**, 223 (1998).
[16] R. Colin, C. Dreze, and M. Steinhauer, Can. J. Phys. **61**, 641 (1983).
[17] P. F. Bernath, A. Shayesteh, K. Tereszchuk, and R. Colin, Science **297**, 1323 (2002).